Slip on an Impermeable Fault in a Fluid-Saturated Rock Mass

J. W. Rudnicki

Reprinted from *Earthquake Source Mechanics*
Geophysical Monograph 37 (Maurice Ewing 6)

SLIP ON AN IMPERMEABLE FAULT IN A FLUID-SATURATED ROCK MASS

J.W. Rudnicki

Department of Civil Engineering Northwestern University Evanston, Illinois 60201

Abstract. Previous solutions for slip in elastic fluid-saturated rock masses are appropriate for permeable faults because they assume no change in pore fluid pressure on the fault (slip) plane. Faults in situ are, however, often barriers to fluid flow, possibly because they contain much clay or very fine-grained gouge material. Here, the solution for a dislocation suddenly emplaced on an impermeable fault is used to analyze coupled deformation diffusion effects for impermeable faults. In contrast to predictions for the permeable fault, the shear stress induced by sudden slip on an impermeable fault does not decay monotonically in time from the undrained (instantaneous) value to the drained (long-time) value, but instead, first rises to a peak in excess of the undrained value by about 20% of the difference between the drained and undrained values. This rise in shear stress suggests that coupling between deformation and diffusion is initially destabilizing. Using two opposite signed dislocations to simulate a finite length fault suggests that the rise in shear stress occurs for 1.5 to 15 days for a fault 4 km in length and diffusivities of 0.1 m^2/s to 1.0 m^2/s. A characteristic time, defined as the time needed for the shear stress on the fault to decay to one-half of its long-time value, is $a^2/4c$ for the impermeable fault compared with $a^2/16c$ for the permeable fault where a is half the fault length and c is the diffusivity. Consequently, diffusive reloading of the fault, suggested as a contributor to aftershocks, does not begin immediately and occurs much more slowly for the impermeable fault. The pore pressure change on the impermeable fault is not zero as for the permeable fault, but is discontinuous and the values are opposite in sign on different sides of the fault. For the permeable fault, the position of the maximum pore pressure change moves away from the fault with time, but the maximum pore pressure change for the impermeable fault is always located at the dislocation.

Introduction

The diffusion of pore fluid induced by slip on a fault can introduce time-dependence into the response of the material surrounding the fault. This time-dependence has been suggested as playing a role in several processes associated with faulting: generation and migration of aftershocks [Nur and Booker, 1972; Booker, 1974], stability of precursory slip [Rudnicki, 1979], fault creep [Rice and Simons, 1976], earthquake swarms [Johnson, 1979] and response of water-wells to propagating creep events [Roeloffs and Rudnicki, 1985]. The solutions that have been used to analyze the coupling between fluid diffusion and fault slip and to interpret relevant field observations are appropriate for permeable faults. There is, however, considerable geological evidence that faults in situ can act as barriers to fluid flow possibly because the fault zones contain much fine-grained material or clay gouge [Wang and Lin, 1978; Wu et al., 1975]. In such cases it is more appropriate to model the fault as impermeable. This paper describes the solution for a shear dislocation suddenly introduced on an impermeable fault plane in a linear elastic, fluid-infiltrated solid. This solution is obviously a crude model for fault slip in the earth's crust. Nevertheless, comparison of this solution with that obtained for a permeable fault [Booker, 1974; Rice and Cleary, 1976] suggests differences in coupled deformation-diffusion effects for permeable and impermeable faults. These differences may be important in assessing the significance of coupled deformation-diffusion effects in fault processes and in designing proper strategies for their observation. Of course a more elaborate model is necessary for detailed analysis of the fault processes that have been mentioned, i.e., slip stability, aftershocks, etc. Such models can, however, be constructed by superposition of the dislocation solution.

This paper does not describe the details of the solution method, but instead concentrates on the results for two quantities of primary interest in fault problems: the shear stress induced on the fault plane and the pore fluid pressure. Differences with the corresponding quantities for the permeable fault are emphasized and the implications of these differences for fault processes are discussed.

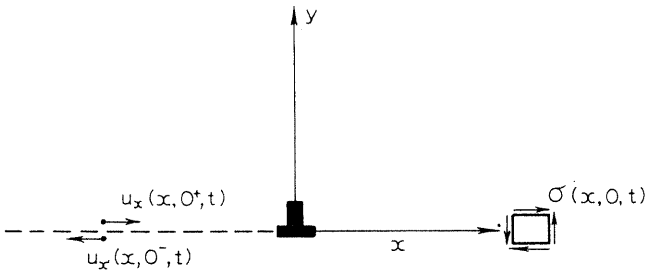

Fig. 1. Geometry of a plane strain shear dislocation. The dislocation corresponds to sudden introduction of a discontinuity in the x-direction displacement on the negative x-axis.

Governing Equations

The governing equations for plane strain deformation (in xy plane) of a linear, fluid-infiltrated, porous elastic material can be written in terms of the stresses σ_{xx}, σ_{xy}, and σ_{yy} and the pore fluid pressure p as follows:

$$\partial\sigma_{xx}/\partial x + \partial\sigma_{xy}/\partial y = 0 \qquad (1)$$

$$\partial\sigma_{xy}/\partial x + \partial\sigma_{yy}/\partial y = 0 \qquad (2)$$

$$\nabla^2(\sigma_{xx} + \sigma_{yy} + 2\eta\, p) = 0 \qquad (3)$$

$$(c\,\nabla^2 - \partial/\partial t)\,[\sigma_{xx} + \sigma_{yy} + (2\eta/\mu)p] = 0 \qquad (4)$$

where c is a diffusivity, $\mu = (\nu_u - \nu)/(1 - \nu)$, and $\eta = 3(\nu_u - \nu)/2B(1 + \nu)(1 - \nu_u)$. The Poisson's ratios ν and ν_u govern drained (slow) and undrained (rapid) deformation, respectively, and B is the ratio of pore fluid pressure to mean normal compression induced during an increment of undrained response. The first two equations express equilibrium in the absence of body forces and the third compatibility of strains. The diffusion equation (4) results from combining Darcy's law and conservation of fluid mass and using (3). The quantity in square brackets is proportional to the fluid mass content per unit volume of porous solid. Rice and Cleary [1976] have given a full discussion of these equations and have tabulated values of the material constants (also, see Rudnicki [1985]). These equations were originally derived in a different form by Biot [1941] and are equivalent to those studied by Booker [1974], although he chooses to express them in terms of displacements and restricts consideration to incompressible constituents. This restriction corresponds to $\nu_u = 1/2$ and $B = 1$.

The introduction of a shear dislocation at the origin corresponds to slitting the negative x-axis and creating a discontinuity in the x-direction displacement u_x (Figure 1). Let $\delta(x, t)$ be the displacement discontinuity defined by

$$\delta(x, t) = u_x(x, 0^+, t) - u_x(x, 0^-, t) \qquad (5)$$

where the notation is intended to indicate that u_x is to be evaluated on the positive and negative sides of the x-axis. For the sudden introduction of a shear dislocation of magnitude b at the origin

$$\delta(x, t) = b\, H(-x)\, H(t) \qquad (6)$$

where H(...) is the unit step function. Because the problem is antisymmetric about the x-axis, it is possible to restrict consideration to the upper half-plane $y > 0$ with boundary conditions applied to $y = 0$. Thus, (5) can be expressed as

$$\delta(x, t) = 2u(x, 0^+, t) \qquad (7)$$

Because of antisymmetry and continuity of tractions across $y = 0$, σ_{yy} is zero on the fault plane:

$$\sigma_{yy}(x, 0, t) = 0 \qquad (8)$$

Darcy's law states that the fluid mass flux is proportional to the gradient of pore fluid pressure. Consequently, for an impermeable fault plane the pore pressure satisfies the following condition:

$$\frac{\partial p}{\partial y}(x, 0, t) = 0 \qquad (9)$$

In the previous solutions due to Booker [1974] and Rice and Cleary [1976], the pore pressure was assumed to be continuous across the fault plane. Because of antisymmetry, the value of p on the fault plane is then required to be zero. Obviously, $\partial p/\partial y$ will not be zero on the fault plane in this case, corresponding to fluid flow across the fault plane. Hence, these solutions are appropriate for a permeable fault. For an impermeable fault, the pore pressure need not be continuous across the fault, but by antisymmetry the values on opposite sides of the fault are still required to be equal in magnitude and opposite in sign.

The governing equations (1), (2), (3), and (4) are expressed in terms of the stresses and pore fluid pressures. Consequently, it is convenient to convert (6) and (7) to conditions on the stresses. The constitutive relation for the strains of the solid matrix $\varepsilon_{\alpha\beta}$ in terms

of the stresses and pore fluid pressure is as follows:

$$2G\varepsilon_{\alpha\beta} = \sigma_{\alpha\beta} - \nu(\sigma_{xx} + \sigma_{yy})\delta_{\alpha\beta} + 2\eta(1-\nu)p\delta_{\alpha\beta} \quad (10)$$

where $\alpha,\beta = x,y$ and $\delta_{\alpha\beta}$ is the Kronecker delta. The strains are related to the displacements by

$$\varepsilon_{\alpha\beta} = \frac{1}{2}\left(\partial u_\alpha/\partial x_\beta + \partial u_\beta/\partial x_\alpha\right) \quad (11)$$

Substituting (11) into (10) and evaluating on $y = 0$ for $\alpha = \beta = x$ yields

$$G\frac{\partial \delta}{\partial x}(x, t) = \sigma_{xx}(1 - \nu) + 2\eta(1 - \nu)p \quad (12)$$

where (7) and (8) have been used. Differentiating (6), substituting into (12) and solving for σ_{xx} yields

$$\sigma_{xx}(x,0,t) = -\frac{G\,b}{(1-\nu)}\,\delta_{DIRAC}(x)\,H(t) - 2\eta\,p(x,0,t) \quad (13)$$

where δ_{DIRAC} is the Dirac delta function. The details of the solution method will not be given here but the general approach was to use the Laplace transform on time and the Fourier transform on x. Expressions for the complete stress and pore pressure fields have been obtained, but these are cumbersome and will not be displayed. Two quantities of most interest, the pore fluid pressure and the induced shear stress on the fault plane, are, however, given by relatively simple expressions and these are discussed in the following sections.

Shear Stress on the Fault Plane

The shear stress on the fault plane ($y = 0$) due to sudden introduction of a unit dislocation at the origin corresponding to left-lateral slip is given by

$$\sigma_{xy}(x, 0, t) = \frac{G\,b}{2\pi(1 - \nu_u)x}\,F\left[x^2/(4ct)\right] \quad (14)$$

The time dependence of the solution is expressed by the function F:

$$F\left[\xi\right] = 1 - \mu\left[2e^{-\xi} - \xi^{-1}(1 - e^{-\xi})\right] \quad (15)$$

where $\mu = (\nu_u - \nu) / (1 - \nu)$. At $t = 0^+$, immediately after the introduction of the dislocation, $\xi = \infty$, $F = 1$ and (14) reduces to the usual elasticity expression based on the undrained Poisson's ratio. At long times, $t \to \infty$, ξ approaches zero and $F[0] = (1 - \nu_u) / (1 - \nu)$. Thus, (14) reduces to the usual elasticity expression based on the drained value of Poisson's ratio. This behavior is identical to that for the dislocation introduced on the permeable fault. The time dependence at intermediate times is, however, much different. For comparison, the function expressing the time dependence of the induced shear stress for a dislocation on a permeable fault is given by [Rice and Cleary, 1976]

$$F_p[\xi] = 1 - \mu\,\xi^{-1}(1 - e^{-\xi}) \quad (16)$$

where the subscript p denotes the permeable fault. Figure 2 plots the following quantity

$$\frac{\sigma_{xy}(x, 0, t) - \sigma_{xy}(x, 0, \infty)}{\sigma_{xy}(x, 0, 0) - \sigma_{xy}(x, 0, \infty)} \quad (17)$$

against $4ct/x^2$ for the permeable and impermeable fault; this is the same as a plot of F and F_p against the reciprocal of their arguments. As shown, the induced shear stess for the permeable fault decays monotonically with time whereas that for the impermeable fault first rises above the undrained value before decaying to the drained value. The height of the peak above the undrained value is about 20% of the difference between undrained and drained values. To estimate the time scale of the changes in shear stress, two dislocations of opposite sign can be used to simulate a finite length fault. Rice [1980] suggests placing the dislocations at the centroids $x = \pm 2a / \pi$ of the slip distribution caused by a uniform stress drop on a fault of length 2a. The time-dependent stress drop is then given approximately by

$$\Delta\tau \approx (\Delta\tau)_{t=o^+}\,F[a^2 / \pi^2\,ct] \quad (18)$$

Figure 3 plots the stress drops in nondimensional form for both the permeable and impermeable faults against ct/a^2. As expected from Figure 2, the stress drop for the impermeable fault continues to decrease for a time after the imposition of the slip, but then increases and eventually reaches the drained value. The minimum in the stress drop for the impermeable fault occurs at $ct/a^2 \approx 0.0325$. For a fault length 2a = 4 km and a diffusivity $c = 0.1\ m^2/s$, a value suggested by Rice and Simons [1976] as representative of field conditions, $t \approx 15$ days. If the diffusivity $c = 1.0\ m^2/s$, then $t \approx 1.5$ days. The stress drop for the permeable fault reaches half of its long-time value when $ct/a^2 \approx 0.0625$ whereas the stress drop for the impermeable fault does not reach half its long time value until $ct/a^2 \approx 0.2425$. For a 2a = 4 km and $c = 0.1\ m^2/s$ these values correspond to approximately 30 days and 112 days.

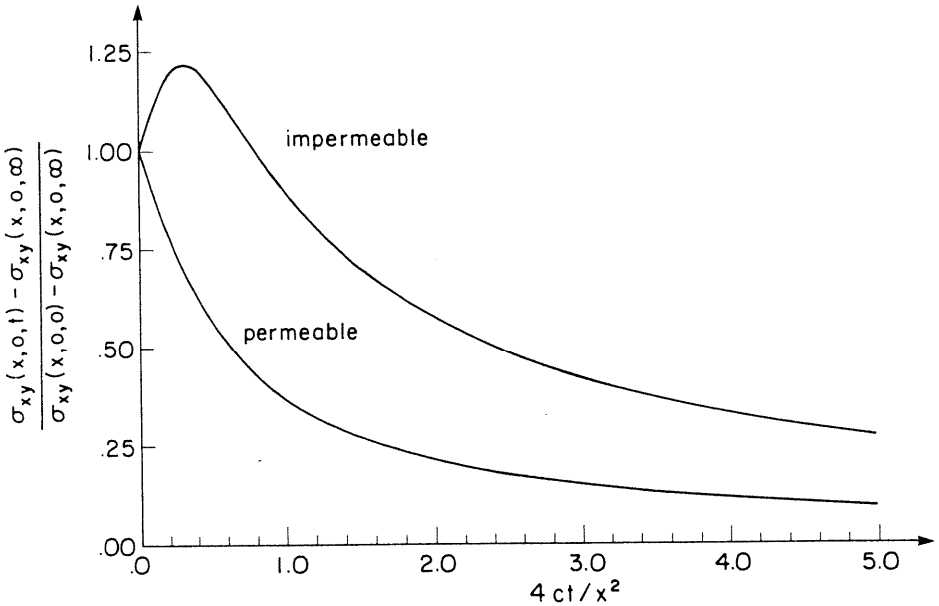

Fig. 2. Time dependence of the shear stress at a fixed position on the x-axis as a function of the nondimensional time ct/x^2 where c is the diffusivity.

The differences in the fault-plane shear stress solutions for the permeable and impermeable faults have implications for several fault processes. First consider that the slip modelled by the dislocations is emplaced seismically. The solution for the permeable fault states that the shear stress induced on the fault plane has its highest value, the undrained value, immediately after slip occurs ($t = 0^+$), and then decays monotonically to the drained value. On the other hand, the solution for the impermeable fault indicates that the induced shear stress will rise from its value immediately after slip is emplaced for a period on the order of days. This means that the effect of coupling between deformation and diffusion is initially destabilizing for the impermeable fault. It is possible that this increase could trigger additional slip. Also, although the shear stress

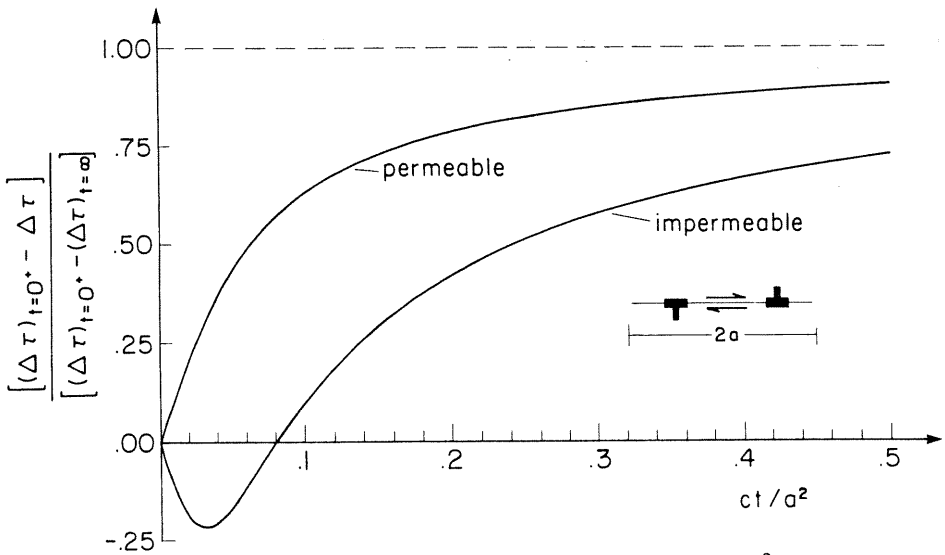

Fig. 3. Stress drop versus time divided by the diffusion time a^2/c for a fault of length 2a. Two dislocations of opposite sign are used to simulate a finite length fault. The increase of the stress drop with time is accompanied by diffusive reloading of the fault.

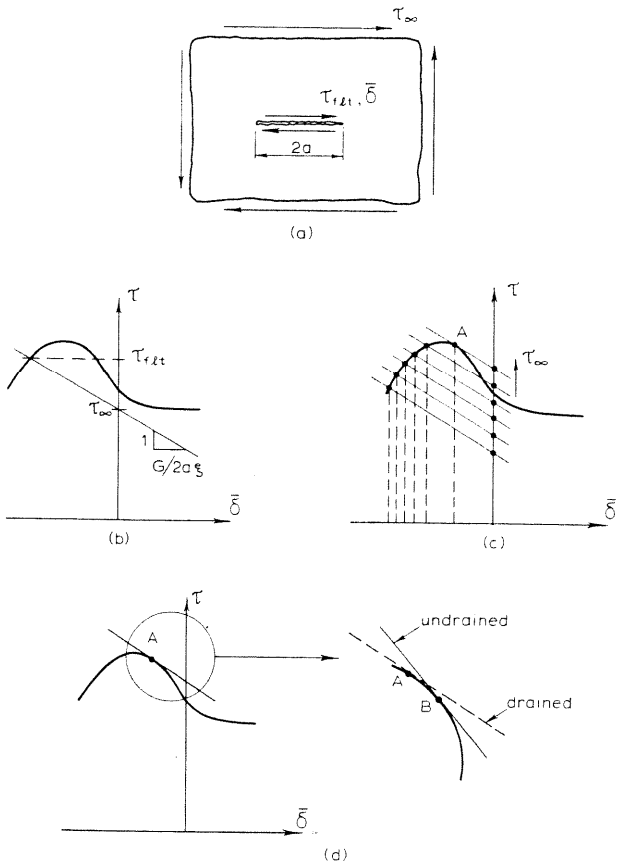

Fig. 4. Graphical construction originated by Rice [1979] for illustrating fault slip instability. (a) Fault of length 2a sustains a shear stress τ_{flt} and average slip $\bar{\delta}$. The fault is loaded by far-field stresses τ_∞. (b) The solution for τ_{flt} and $\bar{\delta}$ corresponding to a value of τ_∞ is given by the intersection of the τ_{flt} versus $\bar{\delta}$ stiffness relation and a straight line representing the effective unloading stiffness of the surrounding material. The slope of this line is minus $G/2a\xi$ where ξ depends on the geometry (e.g. plane strain versus axisymmetry) and the Poisson's ratio of the surrounding material. (c) At point A further increase in τ_∞ cannot be accommodated by quasi-static response. Note that the increments in $\bar{\delta}$ corresponding to equal increments of τ_∞ increase as point A is approached. (d) Delay of instability by coupled deformation-fluid diffusion. Because the unloading stiffness of the material surrounding the fault is greater for more rapid deformation, instability is delayed until B.

on the impermeable fault ultimately decays with time, it remains higher than the shear stress on the permeable fault at any finite, non-zero time.

The differences between the solution for the permeable fault and that for the impermeable fault also require some reassessment of inferences by Nur and Booker [1972] and Booker [1974] (also, discussed by Rice and Cleary [1976] and Rice [1980]) on the possible effects of coupled deformation and diffusion on aftershock processes. These authors noted that the solution for the permeable fault implies that the stress drop accompanying imposition of a fixed amount of slip decreases in time within the slipped region but increases outside of it. Consequently, the total shear stress increases in time within the slipped region but decreases outside it. As explained by Rice [1980], this is consistent with aftershock activity that is confined to the slipped region rather than the presumably more highly stressed surrounding region and is controlled by a time-dependence shown in Figure 3. Because the stress drop for the impermeable fault initially continues to drop after introduction of the dislocation and then rises more slowly than for the permeable fault, one would expect reloading of an impermeable fault to occur more slowly than for a permeable fault. If the time at which the shear stress drop reaches half its long-time value is regarded as characteristic of the duration of aftershock activity, then this time scale is approximately four times as long for the impermeable fault although no aftershock activity would be expected in the period during which stress drop is decreasing for the impermeable fault.

The solution also suggests that predictions of coupled deformation-diffusion effects on precursory slip may be different for permeable and impermeable faults. Figure 4 shows the graphical construction originated by Rice [1979] and used by Rudnicki [1979] to discuss the stabilizing effects due to coupled deformation-diffusion in the material surrounding a permeable fault. Initially, the material surrounding the fault responds in drained fashion because slip occurs slowly, by comparison to the diffusion time, under the action of increasing tectonic stress τ_∞ (Figure 4b, c). As instability, predicted on the basis of the drained response, is approached (point A in Figure 4c, 4d), the accelerating fault slip induces the shorter time response of the material surrounding the fault. Because this response is stiffer than the drained response, instability is delayed. The response to instantaneous slip is undrained and, hence, instability occurs when the slope of the τ_{flt} versus $\bar{\delta}$ curves equals the undrained unloading stiffness of the surrounding material (B in Figure 4d). Because of the differences in the time dependence of fault stress for the permeable and impermeable faults, the transition from drained to undrained behavior will be different. Rudnicki's [1979] analysis of the permeable fault predicted that the delay in the onset of fault instability due to coupled deformation-fluid diffusion effects occurred over such a short-time period that detection would be difficult. Whether the different time-dependent response of the impermeable fault gives rise to a longer precursory period is unclear.

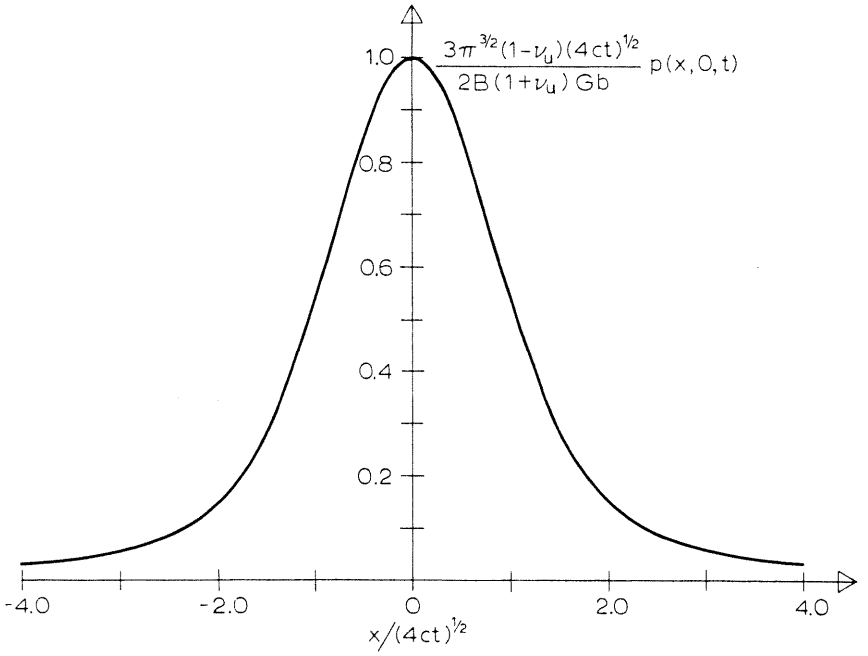

Fig. 5. Pore pressure, in nondimensional form, induced on the positive side ($y = 0^+$) by a sudden dislocation of an impermeable fault. The pore pressure induced on the other side of the fault ($y = 0^-$) is equal in magnitude and opposite in sign to that shown here.

Pore Fluid Pressure

For the impermeable fault the induced pore fluid pressure is given by

$$p(x, y, t) = \frac{B(1 + \nu_u)Gb}{3\pi(1 - \nu_u)} \{(y/r^2)\,\mathrm{erf}\,[y/(4ct)^{1/2}] + (2x/\pi^{1/2} r^2)e^{-y^2/4ct}\,\mathrm{Daw}\,[x/(4ct)^{1/2}]\} \tag{19}$$

where $r^2 = x^2 + y^2$, erf(ξ), is the error function defined [Abramowitz and Stegun, 1964, 7.1.1] as

$$\mathrm{erf}(\xi) = (2/\pi^{1/2}) \int_0^{\xi} e^{-\alpha^2}\, d\alpha \tag{20}$$

and Daw(ξ), is Dawson's integral, defined as [Abramowitz and Stegun, 1964]

$$\mathrm{Daw}(\xi) = e^{-\xi^2} \int_0^{\xi} e^{\alpha^2}\, d\alpha \tag{21}$$

Equation (19) gives the pore pressure in the half-plane $y > 0$; the values in the lower half-plane $y < 0$ are the negative of those in (19).

Figure 5 plots the non-dimensional pore pressure P

$$P = \frac{3\pi^{3/2}(1 - \nu_u)(4ct)^{1/2}}{2B(1 + \nu_u)\,Gb}\,p \tag{22}$$

on the positive side of the fault plane ($y = 0^+$) for a fixed time $t > 0$. Because the fault plane is impermeable, the pore pressure is discontinuous and the values on the lower side of the fault plane, $y = 0^-$, are the negative of those shown in Figure 5. Increases in pore pressure decrease the effective compressive stress on the fault, that is, the total compressive stress minus the pore fluid pressure and promote further slip. Consequently, a measure of the tendency of the induced stress changes to promote slip is

$$\psi(x, t) = \frac{2\pi(1 - \nu_u)}{Gb}\,[\sigma_{xy}(x, 0, t) + \phi\, p(x, 0, t)] \tag{23}$$

where ϕ is a friction coefficient (because of (8), the normal stress on the fault is constant). This quantity is plotted against $x/(4ct)^{1/2}$ in Figure 6 for the positive side of the fault ($y = 0^+$). The dashed curve shows the shear stress only. The values of ψ on $y = 0^+$ lie above it. This suggests that slip is promoted on the side of the fault with positive pore pressure and inhibited on the side with negative pore pressure.

For a finite length fault there will be positive and negative contributions to the pore

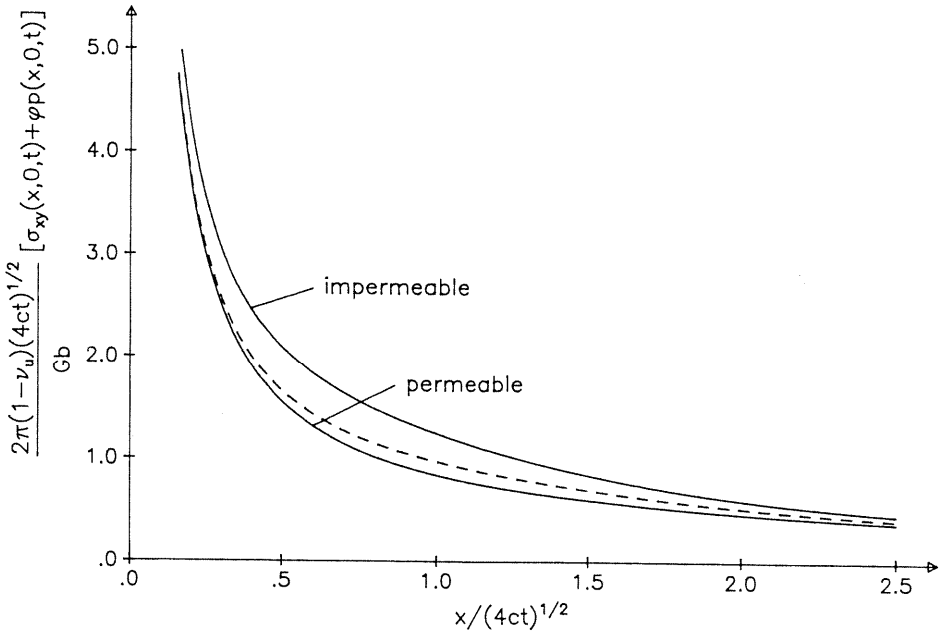

Fig. 6. Combined effect of the shear stress $\sigma_{xy}(x, 0, t)$ and pore fluid pressure $p(x, 0^+, t)$ induced on the positive side ($y = 0^+$) of an impermeable fault. The dashed curve shows $\sigma_{xy}(x, 0, t)$ in nondimensional form for the impermeable fault. Because the pore pressure is zero on the permeable fault the curve labeled "permeable" is $\sigma_{xy}(x, 0, t)$ in nondimensional form. The plot is for $\phi = 0.6$.

pressure on each side of the fault. If the fault is modelled simply as two dislocations of opposite sign, the largest pore pressure changes will occur at the dislocations, near the ends of the fault, and be of opposite sign at the two ends on the same side of the fault. As a specific example, consider a finite length fault with the left lateral slip geometry shown in Figure 1; the pore pressure will increase on $y = 0^+$ near the right end and on $y = 0^-$ near the left end. A manifestation of this prediction might be the presence of transverse subsidiary faults in the regions of pore pressure increase, but not in the regions of decrease. Note, however, that the uncoupled elasticity solution predicts an increase in compressive mean stress, in the regions of pore pressure increase.

The curve labeled "permeable" in Figure 6 is the shear stress on the permeable fault; because the pore pressure is zero on the permeable fault, ψ is equal to the shear stress. As shown, the shear stress ahead of the dislocation is greater for the impermeable fault.

Figure 7 shows contours (solid lines) of the nondimensional pore pressure (22) for $y > 0$ at a fixed time $t > 0$. As required by the condition of no flow across the fault, the contours of constant pore pressure intersect the fault at right angles. Because flow occurs in directions of decreasing pore fluid pressure, the flow near the fault is away from the origin. For comparison the pore pressure induced by sudden introduction of a dislocation on a permeable fault is [Rice and Cleary, 1976]

$$p = \frac{B(1 + \nu_u)b}{3\pi(1 - \nu_u)} G \frac{y}{r^2} [1 - \exp(-r^2/4ct)] \quad (24)$$

Contours of this pore pressure in the same nondimensional form are shown as dashed lines in Figure 7. As noted by Booker [1974], the maximum pore pressure change occurs at a position that diffuses away from the fault with time. In contrast, the maximum pore pressure change for the impermeable fault occurs at the edge of the slip zone and remains there. The contours for the two cases merge away from the fault, but are different near the fault because of the different boundary conditions. In particular, note that the pore pressure changes are much greater near the impermeable fault.

Nur and Booker [1972] have noted that pore pressure changes induced off the fault plane could reduce the effective confining stress and contribute to the occurrence of aftershocks. A proper evaluation of this suggestion would need to consider, in addition, the stress changes at different orientations off the fault plane. Nevertheless, the pore pressure distribution near the fault seems sufficiently different for permeable and impermeable faults that differences in aftershock distribution might be anticipated if

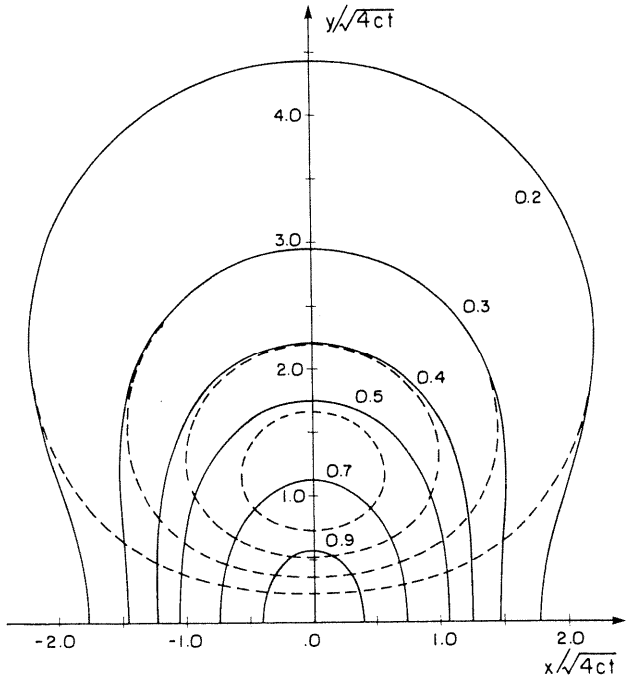

Fig. 7. Comparison of the contours of the non-dimensional pore pressure (22) for permeable (dashed) and impermeable (solid) faults. Plot is for a fixed time not equal to zero.

indeed coupled deformation diffusion effects play a prominent role.

Concluding Discussion

This paper has presented the solution for the shear stress on the fault plane and the pore fluid pressure induced by the sudden introduction of a shear dislocation at the origin. These results have been contrasted with those previously obtained by Booker [1974] and Rice and Cleary [1976] for a permeable fault. The most notable of the differences in the solutions are the larger pore pressure changes near the fault and the increase of the fault plane shear stress over the undrained value for the impermeable fault. A full assessment of the effects of these differences on fault processes, such as aftershocks and slip stability, must await study of fault models more realistic than the suddenly introduced dislocation. Nevertheless, the differences seem great enough that they should be considered in observational as well as theoretical studies of coupled deformation-fluid diffusion effects.

Some preliminary results have also been obtained for the pore pressure induced by a dislocation steadily propagating on an impermeable fault [Roeloffs and Rudnicki, 1984]. As for the stationary dislocation, the results substantially differ from those for the permeable fault [Roeloffs and Rudnicki, 1985]. Specifically, the pore pressure at a fixed distance from the impermeable fault rises more sharply than for the permeable fault and then falls quickly to zero as the dislocation passes, but does not reverse sign, as for the permeable fault. These results are relevant to predictions of the change of water well levels in response to creep events [Wesson, 1981; Lippincott et al., 1985].

A question to be answered is whether coupled deformation-diffusion effects can stabilize propagating slip on an impermeable fault as predicted by Rice and Simons [1976] for a shear crack propagating on a permeable fault. An important feature of their solution is that the neighborhood of the edge of the slip zone always responds in drained fashion because the pore pressure on the fault plane is zero. For the impermeable fault, the pore pressure on the fault plane will not be zero and the effect on stabilization is unknown. One possibility for a destabilizing effect, suggested by the solutions for both the moving and the suddenly introduced dislocations, is that the pore pressure on one side of the fault ahead of the slipping region is increased tending to promote further slip there.

Acknowledgments. I thank J. Rice for suggesting some time ago that I look at this problem and E. Roeloffs for many helpful discussions.

This work was supported by the National Science Foundation and the U.S. Geological Survey.

References

Abramowitz, M. and I.A. Stegun, (Eds.), Handbook of Mathematical Functions, Appl. Math. Ser. 55, National Bureau of Standards, Washington, D.C., 1964.

Biot, M.A., General theory of three-dimensional consolidation, J. Appl. Phys., 12, 155-164, 1941.

Booker, J.R., Time-dependent strain following faulting of a porous medium, J. Geophys. Res., 79, 2037-2044, 1974.

Johnson, C.E., I. CEDAR - an approach to the computer automation of short period local seismic networks; II. Seismotectonics of the Imperial Valley of Southern California, Ph.D. thesis, 332 pp., California Institute of Technology, 1979.

Lippincott, D.K., J.D. Bredehoeft, and W.R. Moyle, Jr., Recent movement on the Garlock fault as suggested by water level fluctuations in a well in Fremont Valley, California, J. Geophys. Res., 90, 1911-1924, 1985.

Nur, A., and J.R. Booker, Aftershocks caused by fluid flow?, Science, 175, 885-887, 1972.

Rice, J.R., Theory of precursory processes in the inception of earthquake rupture, Gerlands Beitr. Geophys., 81, 91-127, 1979.

Rice, J.R., The mechanics of earthquake rupture, in Physics of the Earth's Interior, Proc. Intl. School of Physics "Enrico Fermi," edited by A.M. Dziewonski and E. Boschi, pp. 555-649, North Holland, Amsterdam, 1980.

Rice, J.R., and M.P. Cleary, Some basic stress-diffusion solutions for fluid-saturated elastic porous media with compressible constituents, Rev. Geophys. Space Phys., 14, 227-241, 1976.

Rice, J.R., and D.A. Simons, The stabilization of

spreading shear faults by coupled deformation-diffusion effects in fluid-infiltrated porous solids, J. Geophys. Res, 81, 5322-5334, 1976.

Roeloffs, E., and J.W. Rudnicki, Coupled deformation-pore fluid diffusion effects on fault rupture, Final Technical Report on Contract No. 21818, 30 pp. U.S. Geol. Sur., October, 1984.

Roeloffs, E., and J.W. Rudnicki, Coupled deformation-diffusion effects on water level changes due to propagating creep events, Pure Appl. Geophys, 122, 560-582, 1985.

Rudnicki, J.W., Stabilization of slip on a narrow weakening fault zone by coupled deformation - pore fluid diffusion, Bull. Seismol. Soc. Am., 69, 1011-1026, 1979.

Rudnicki, J.W., Effects of pore fluid diffusion on deformation and failure of rock, in Mechanics of Geomaterials, Proc. IUTAM William Prager Symposium on Mechanics of Geomaterials: Rocks, Concrete, Soils, edited by Z.P. Bazant, pp. 315-347, John Wiley and Sons, New York, 1985.

Wang, C-Y, and W. Lin, Constitution of the San Andreas fault zone at depth, Geophys. Res. Lett., 5, 741-744, 1978.

Wesson, R.L., Interpretation of changes in water level accompanying fault creep and implications for earthquake prediction, J. Geophys. Res, 86, 9259-9267, 1981.

Wu, F.T., L. Blatter, and H. Roberson, Clay gouges in the San Andreas fault system and their possible implications, Pure Appl. Geophys., 113, 87-95, 1975.